Supporting Information

Functional Construction a Water-stable Tb-Coordination Polymer Luminescent Sensor for Highly Selective Detecting Picric Acid in Aquatic Environment

*Wei Liu [a,b], Chengdong Liu [a], Chunyang Chen [c], Xin Huang [a], Weisheng Liu [*a]*

[a.]Key Laboratory of Nonferrous Metals Chemistry and Resources Utilization of Gansu Province, State Key Laboratory of Applied Organic Chemistry and College of Chemistry and Chemical Engineering, Lanzhou University, Lanzhou 730000, China, E-mail: liuws@lzu.edu.cn.

[b.]School of Physical Science and Technology, Lanzhou University, Lanzhou 730000, China.

[c.]College of Earth and Environmental Sciences, Lanzhou University, Lanzhou 730000, China.

Lanzhou 730000 (P.R. China). *E-mail: liuws@lzu.edu.cn. Tel: +86-931-8915151.

College of Earth and Environmental Sciences, Lanzhou University, Lanzhou 730000, China.

Materials and Instrumentation: All solvents and reagents were commercially available A.R. grade and used without further purification unless otherwise noted. Preparation of stock solutions: All the analytic nitro explosives solutions were prepared by separately dissolving each of them DMF with a concentration of 0.1 M . River water samples were taken from Lanzhou section of the Yellow River. Tap water samples were taken from the Second Chemical Building of Lanzhou University. Water samples need to be precipitated for 12 hours before testing and filtered to remove solid insolubles. Luminescence spectra were measured using a Hitachi F-7000 luminescence spectrometer. Fluorescent quantum yieldswere determined by an absolute method using

an integrating sphere on FLS920 of Edinburgh Instrument. UV-visible spectra were recorded using an Agilent Cary 5000 spectrophotometer. The FT-IR spectra were recorded from KBr pellets in the range from 4000 to 400 cm^{-1} on a Bruker VERTEX 70 spectrometer. Powder X-Ray diffraction (PXRD) patterns were collected with a PAN alytical X'Pert Pro Diffractometer operated at 40 kV and 40 mA with Cu Kα radiation. Thermogravimetric analyses (TGA) were obtained on a NETZSCH STA 449 F3 Jupiter® under a N_2 atmosphere. Elemental analyses were performed using an Elementar Analysenesysteme GmbH varioEL cube instrument.

X-ray Structural Crystallography: The single-crystal X-ray diffraction data was collected on an Agilent Super Nova Single Crystal Diffractometer equipped with graphite-monochromatic Mo-Kα source (λ=0.71073 Å). An empirical absorption correction based on a comparison of redundant and equivalent reflections was applied by using SADABS. All of the structures were solved by direct methods using SHELXTL-97[1] and refined by full-matrix least-squares cycles on F^2. All the non-hydrogen atoms were refined anisotropically. The crystal data is listed in Table S1-S3.

Calculations of Luminescent Quantum Yield: Luminescent quantum yield data were measured in the solid state at 298K, and the emission was monitored from 450 to 650 nm. The overall luminescent quantum yields of the solid-state samples were determined by an absolute method using an integrating sphere on FLS920 of Edinburgh Instrument (150 mm diameter, $BaSO_4$ coating) and acquired using the following equation:

$$\Phi_{overall} = (A_H) / (R_{ST} - R_H) \quad (1)$$

where A_H is the area under emission spectrum of the sample and R_{ST} and R_H are diffuse reflectance of the reflecting standard and the sample, respectively.[1]

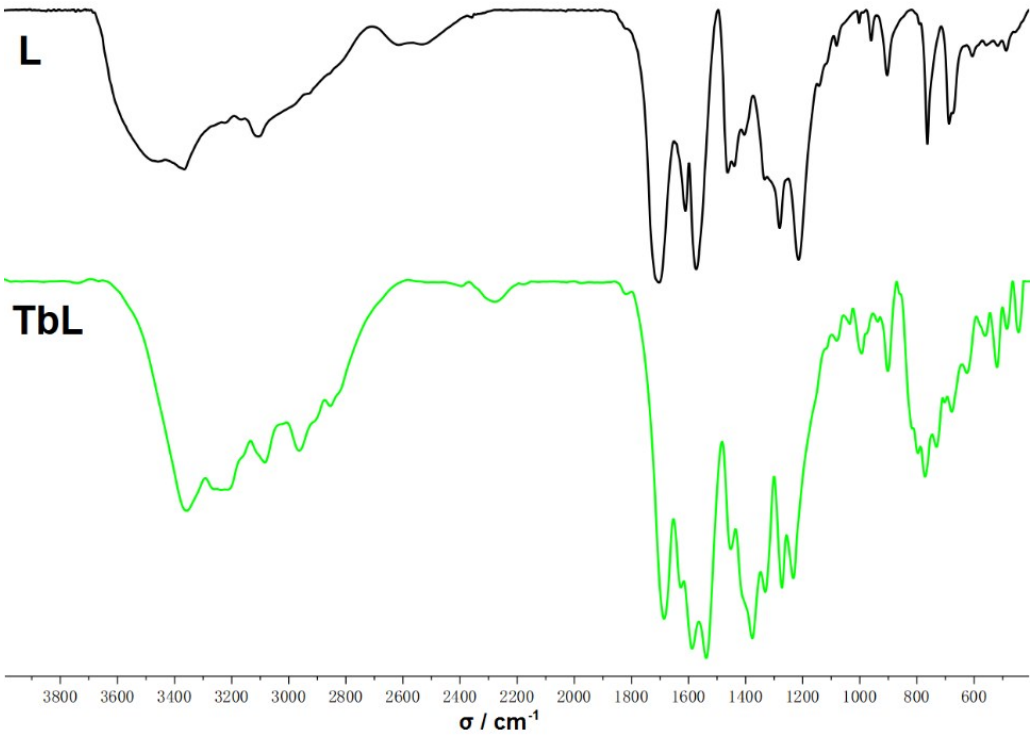

Figure S1. IR spectra of TbL and L.

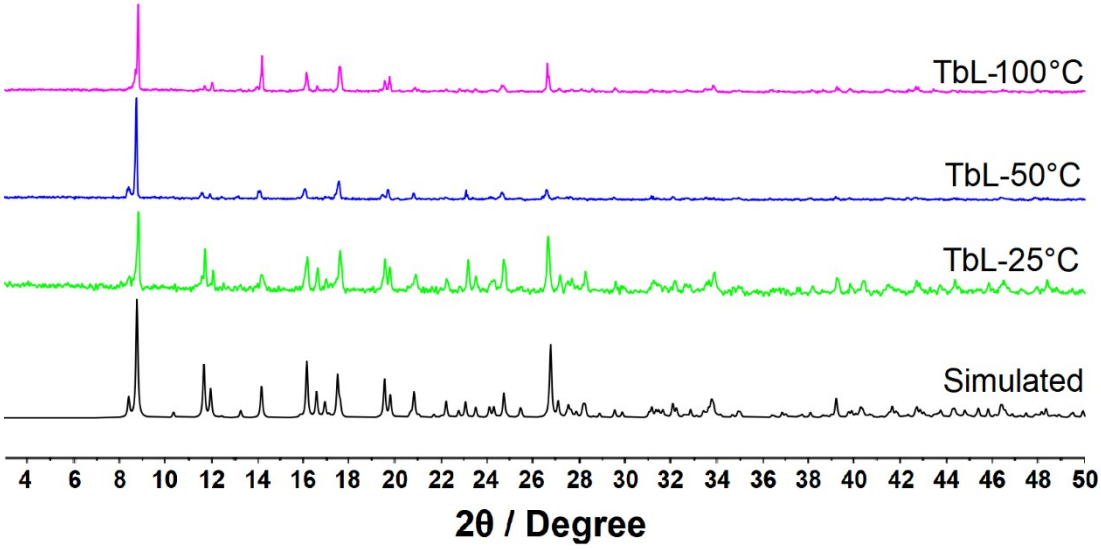

Figure S2. The PXRD of TbL after treatment at different temperatures.

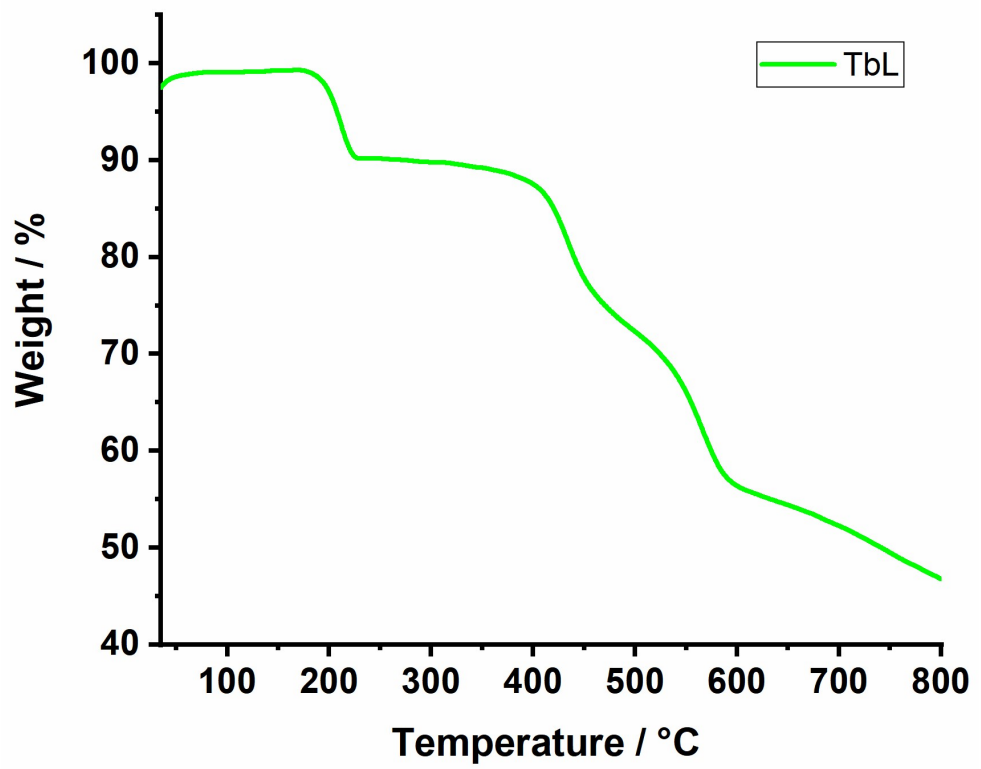

Figure S3. TGA Plot of TbL.

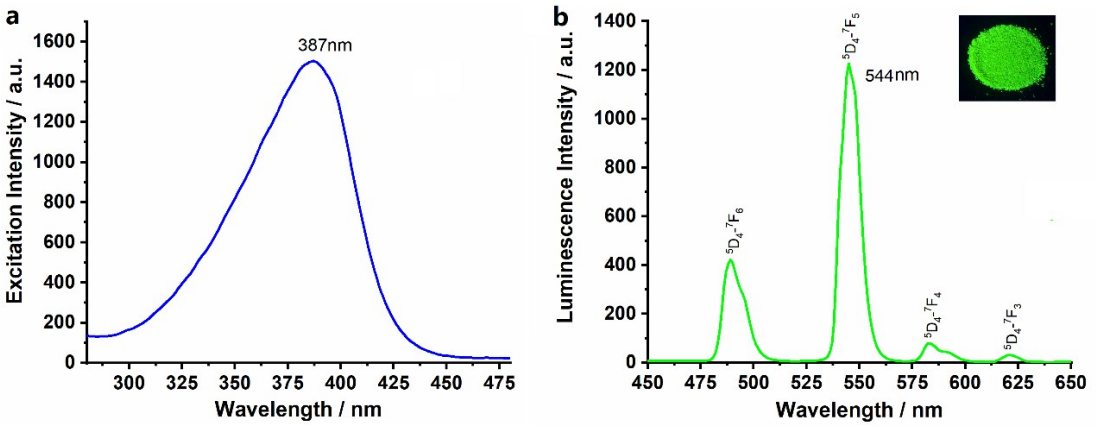

Figure S4. a) The solid-state excitation spectrum of TbL at room temperature (em = 545 nm). b) The solid-state emission spectrum of TbL at room temperature (ex = 387 nm). Insets: the corresponding luminescence pictures under UV-light irradiation of 365 nm.

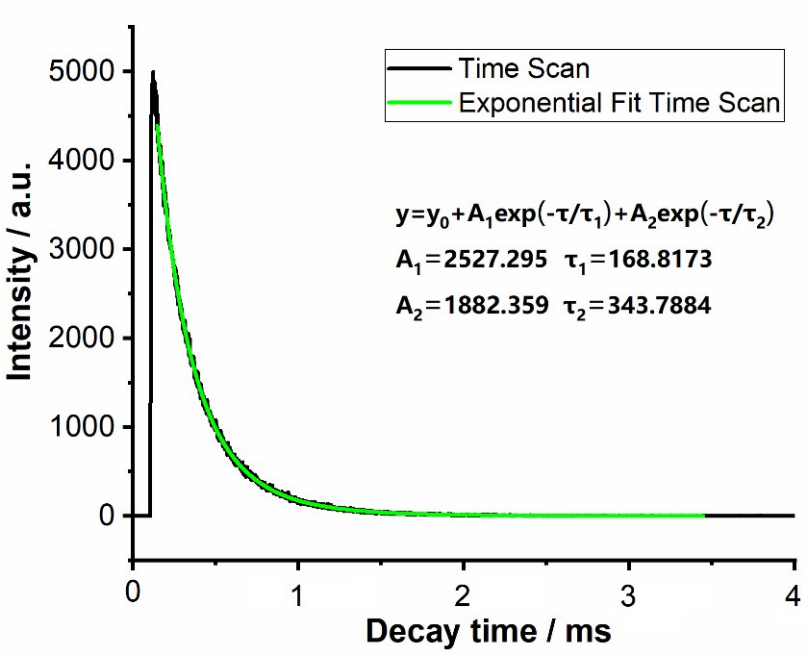

Figure S5. The luminescence decay profiles of TbL.

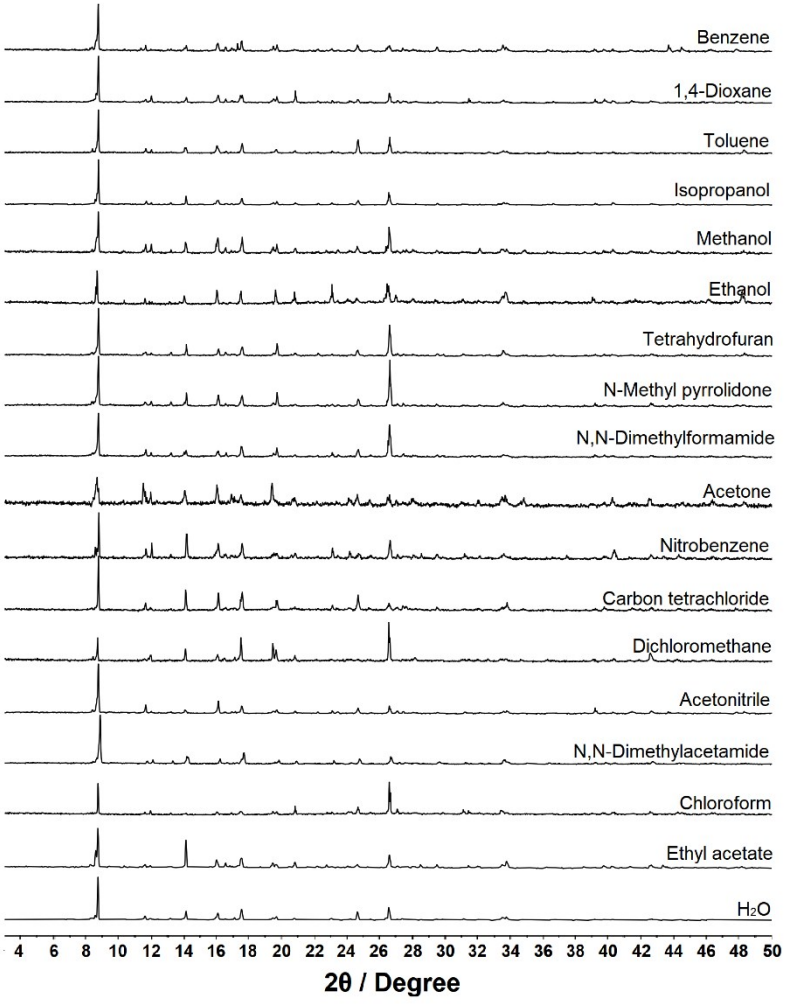

Figure S6. The PXRD of TbL treated with various solvents.

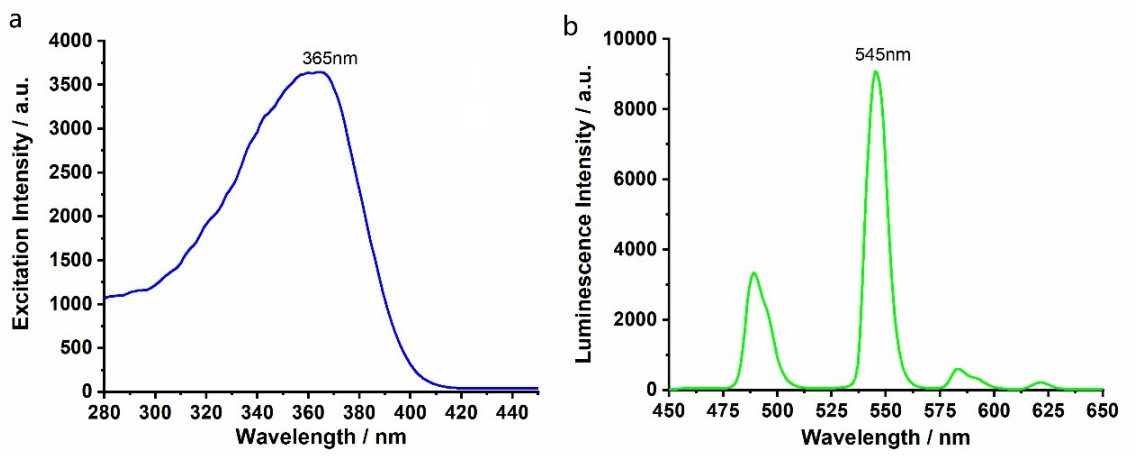

Figure S7. a) The excitation spectrum of TbL in deionized water (em = 545 nm). b) The emission spectrum of TbL in deionized water (ex = 365 nm).

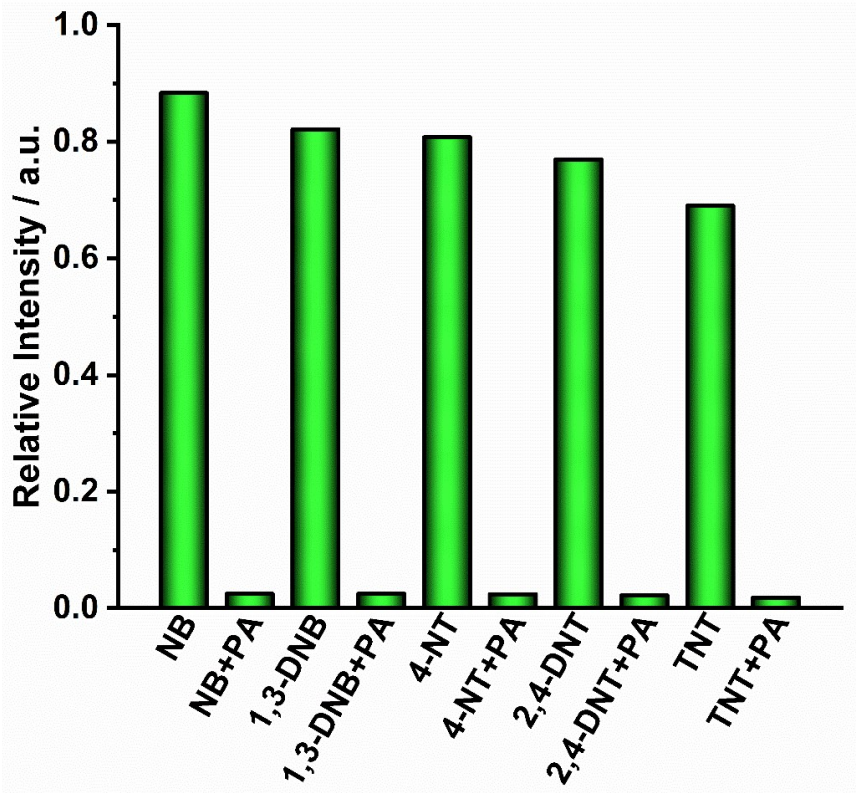

Figure S8. Luminescence responses of TbL to PA (0.5 mM) in the presence of other nitro explosives (0.5 mM) in deionized water (ex = 365 nm).

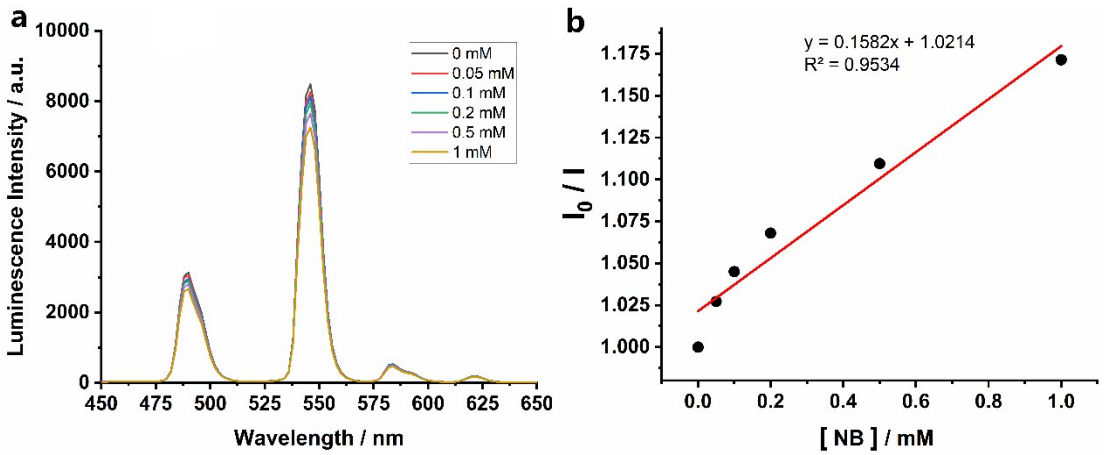

Figure S9. a) Luminescence responses of TbL toward different concentrations of NB (0-1 mM) in deionized water. (ex = 365 nm) b) Stern-Volmer plot of I_0/I versus increasing concentrations of NB.

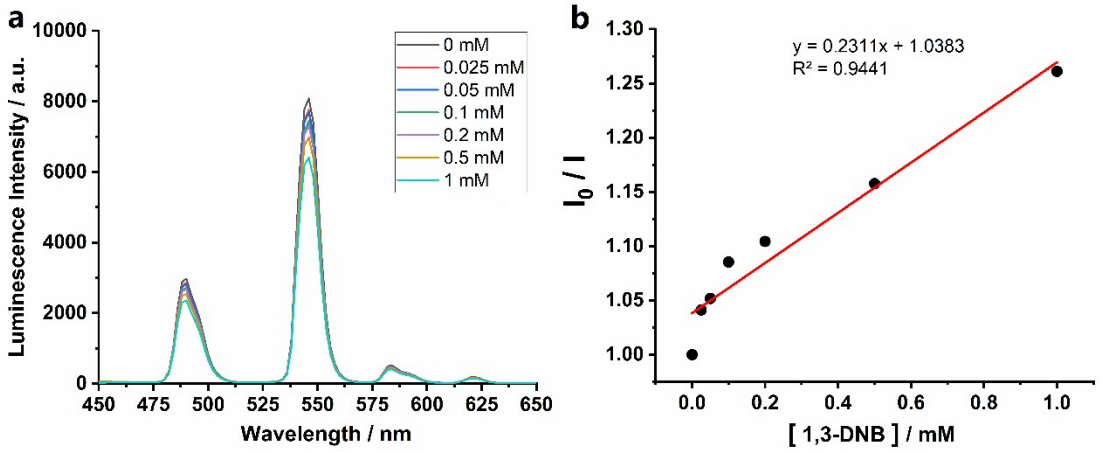

Figure S10. a) Luminescence responses of TbL toward different concentrations of 1,3-DNB (0-1 mM) in deionized water. (ex = 365 nm) b) Stern-Volmer plot of I_0/I versus increasing concentrations of 1,3-DNB.

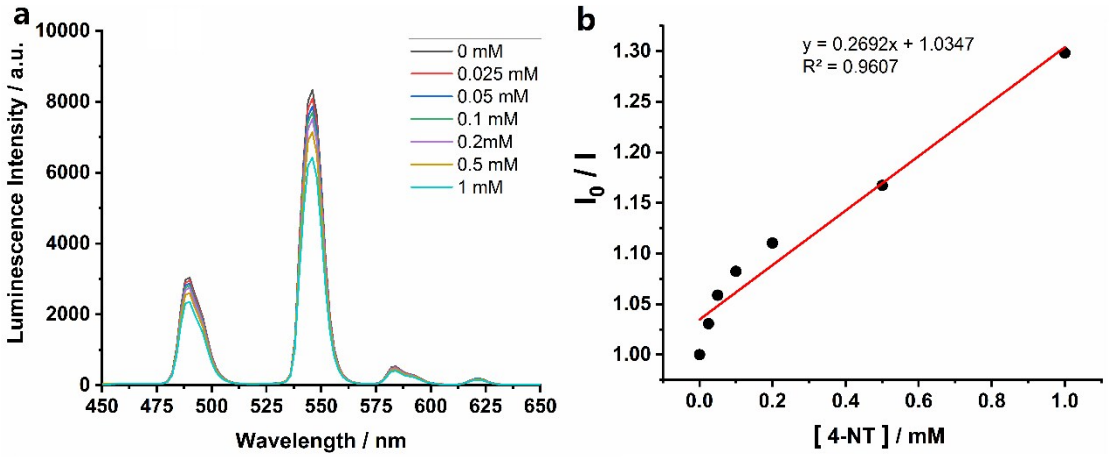

Figure S11. a) Luminescence responses of TbL toward different concentrations of 4-NT (0-1 mM) in deionized water. (ex = 365 nm) b) Stern-Volmer plot of I_0/I versus increasing concentrations of 4-NT.

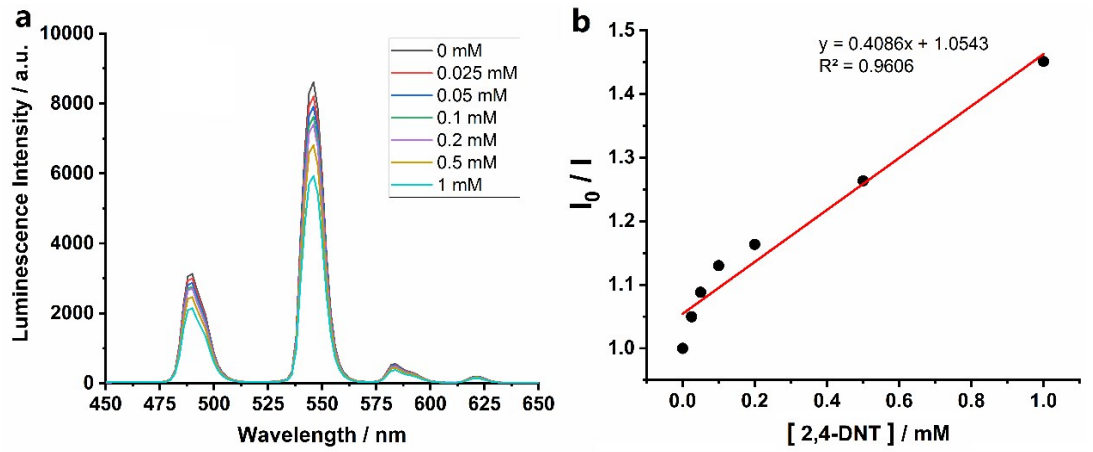

Figure S12. a) Luminescence responses of TbL toward different concentrations of 2,4-DNT (0-1 mM) in deionized water. (ex = 365 nm) b) Stern-Volmer plot of I_0/I versus increasing concentrations of 2,4-DNT.

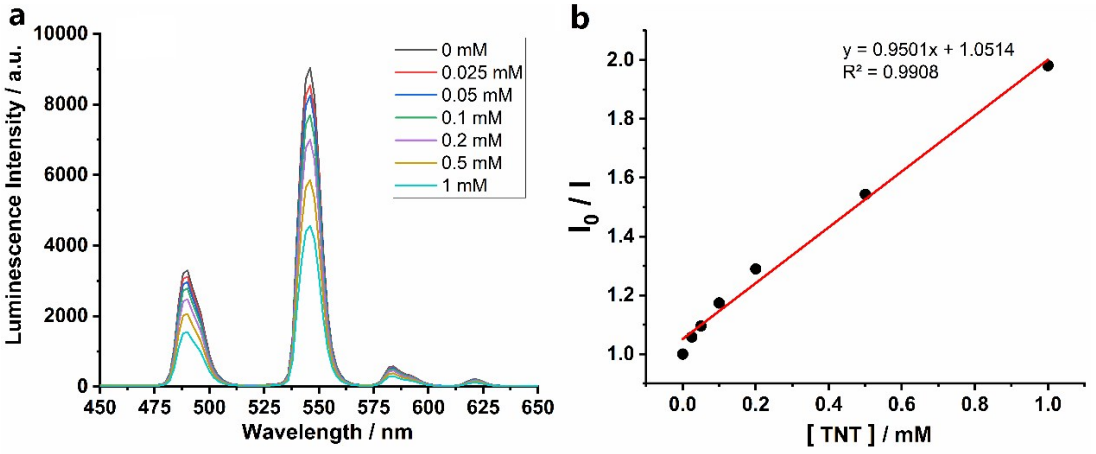

Figure S13. a) Luminescence responses of TbL toward different concentrations of TNT (0-1 mM) in deionized water. (ex = 365 nm) b) Stern-Volmer plot of I_0/I versus increasing concentrations of TNT.

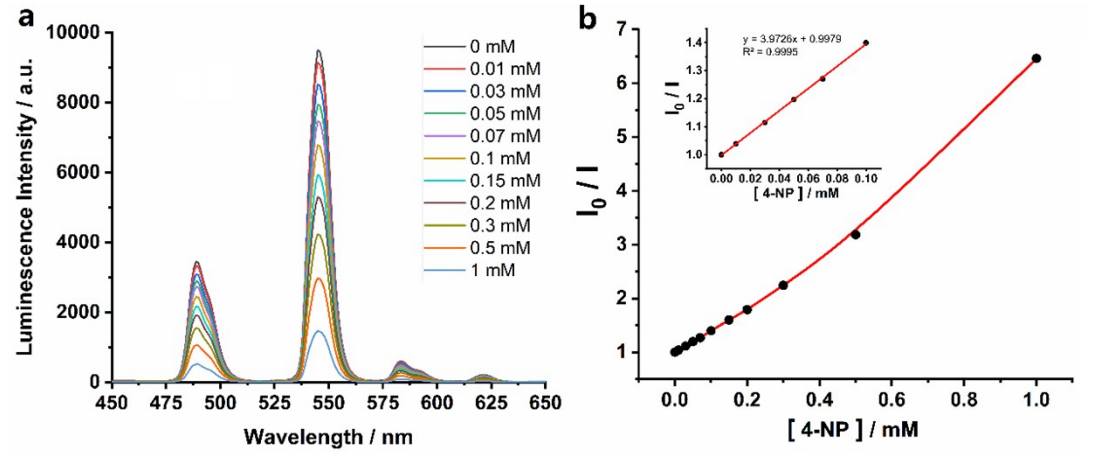

Figure S14. a) Luminescence responses of TbL toward different concentrations of 4-NP (0-1 mM) in deionized water. (ex = 365 nm) b) Stern-Volmer plot of I_0/I versus increasing concentrations of 4-NP.

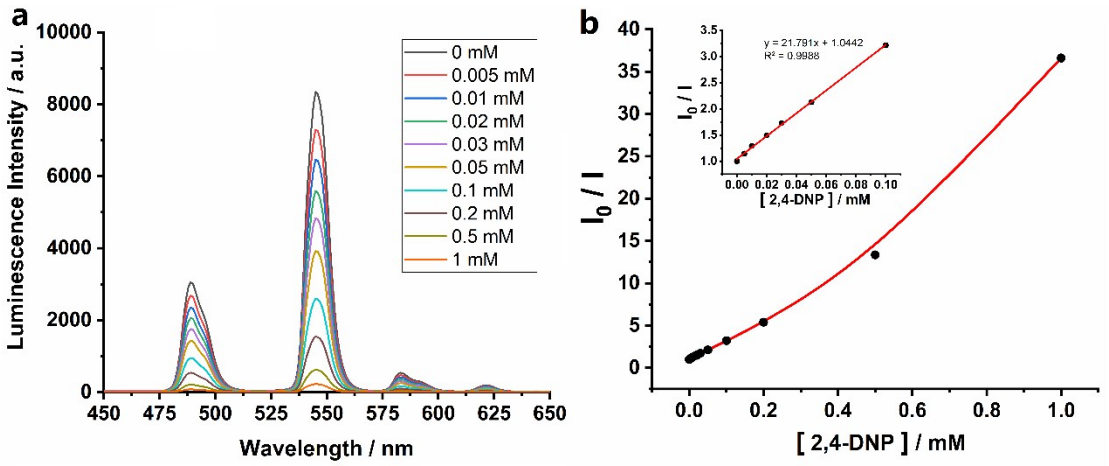

Figure S15. a) Luminescence responses of TbL toward different concentrations of 2,4-DNP (0-1 mM) in deionized water. (ex = 365 nm) b) Stern-Volmer plot of I_0/I versus increasing concentrations of 2,4-DNP.

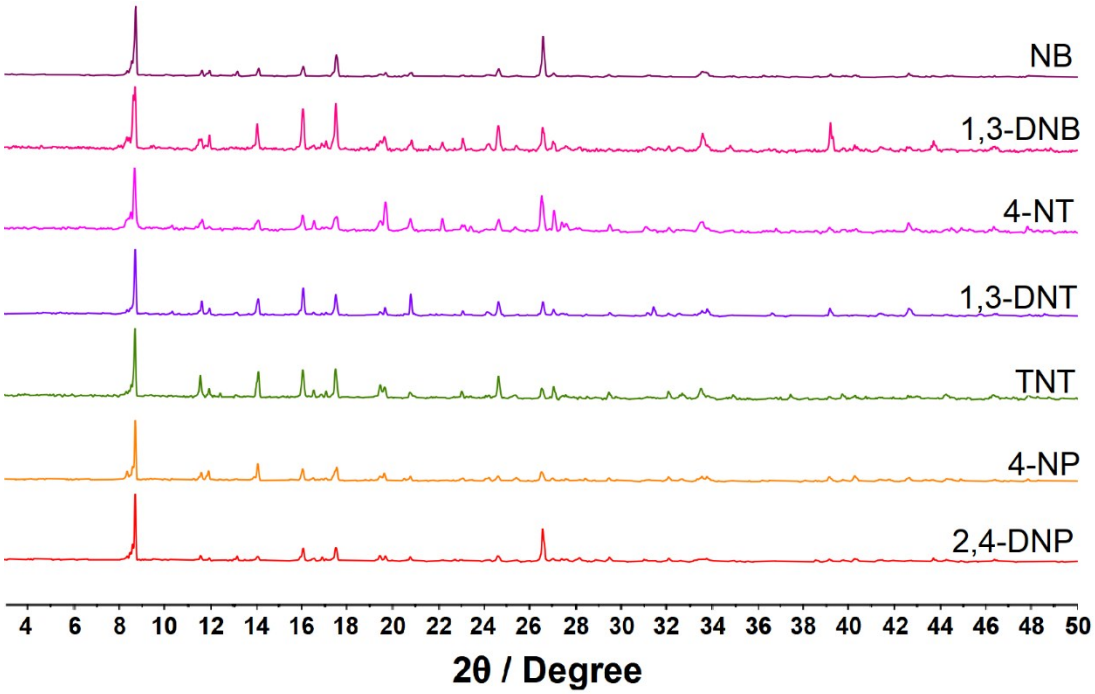

Figure S16. The PXRD patterns of TbL and treated by various analytes. (Obtained after immersing in deionized water with various analytes (1 mM) for 12 h)

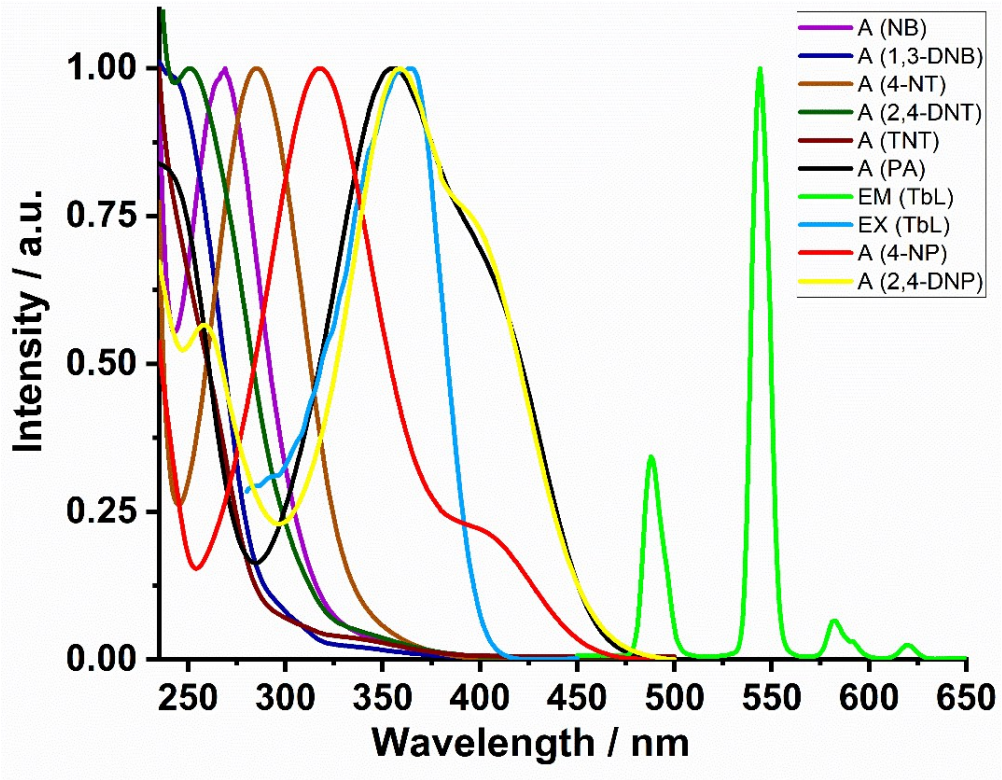

Figure S17. Spectral overlap between normalized excitation spectrum and luminescence spectrum of TbL and normalized absorbance spectra of nitro explosives in deionized water.

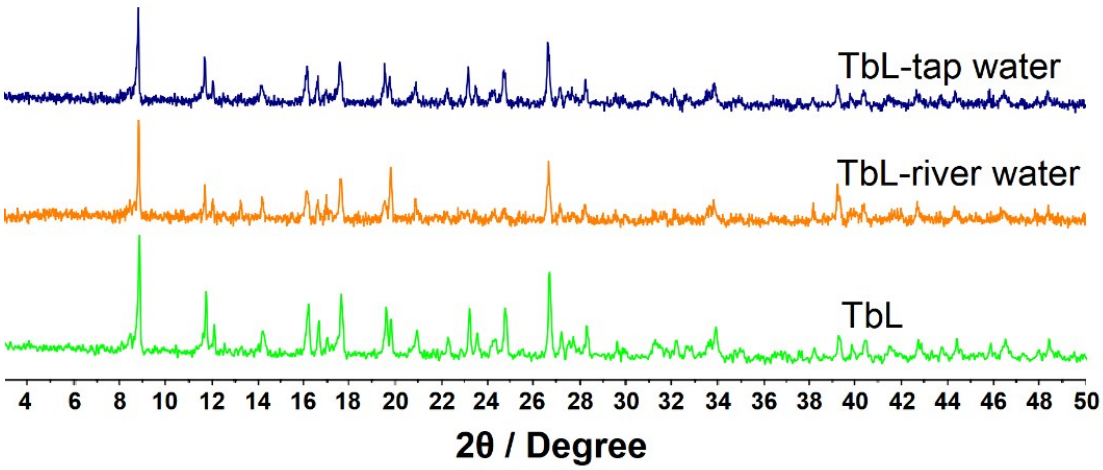

Figure S18. The PXRD patterns of TbL treated by PA. Obtained after immersing in river water solution and tap water solution with PA (0.5 mM) for 12 h

Table S1. Crystal data and structure refinement for TbL.

Compound	TbL
Empirical formula	$C_{17}H_{14}N_2O_{12}Tb$
Formula weight	597.22
Crystal system	monoclinic
Space group	C2/c
a/Å	14.354(3)
b/Å	17.052(2)
c/Å	16.986(2)
α/°	90
β/°	119.674(12)
γ/°	90
Volume/Å^3	3612.2(11)
Z	8
D_{calc} g/cm^3	2.196
F(000)	2328.0
Reflections collected	11668
Data/restraints/parameters	3300/0/292
Goodness-of-fit on F^2	1.075
Final R indexes [I>=2σ (I)]	R_1 = 0.0309, wR_2 = 0.0815
Final R indexes [all data]	R_1 = 0.0341, wR_2 = 0.0835

Table S2. The bond lengths for TbL.

Atom	Atom	Length/Å	Atom	Atom	Length/Å
Tb1	O6	2.302(3)	C27	C28	1.486(5)
Tb1	O5	2.285(3)	C27	C29	1.390(5)
Tb1	O1	2.511(3)	C28	O2	1.279(5)
Tb1	C28	2.882(4)	N14	C21	1.375(5)
Tb1	O21	2.383(3)	N14	C222	1.397(5)
Tb1	O2	2.521(3)	C13	C14	1.498(5)
Tb1	O8	2.347(3)	C24	C25	1.514(5)
Tb1	O9	2.441(3)	C24	C23	1.399(5)
Tb1	O7	2.349(3)	C20	C14	1.397(6)
C26	C27	1.402(5)	N23	C21	1.360(5)
C26	C24	1.386(5)	C14	C15	1.382(6)
O6	C17	1.240(5)	C29	C22	1.389(5)
O12	C21	1.231(5)	C25	O4	1.256(5)
O5	C13	1.249(5)	C25	O3	1.272(5)
O11	C13	1.267(5)	C23	C22	1.400(5)
O1	C28	1.263(5)	C18	C16	1.395(6)

C19	C20	1.399(5)	C15	C16	1.394(6)
C19	N23	1.407(5)	C16	C173	1.475(5)
C19	C18	1.396(5)	O10	C17	1.285(5)

[1]2-X,-Y,-Z; [2]-1/2+X,-1/2-Y,-1/2+Z; [3]-1/2+X,1/2-Y,-1/2+Z

Table S3. The bond angles for TbL.

Atom	Atom	Atom	Angle/°	Atom	Atom	Atom	Angle/°
O6	Tb1	O1	107.45(9)	C26	C27	C28	121.5(3)
O6	Tb1	C28	131.05(10)	C29	C27	C26	120.6(3)
O6	Tb1	O21	117.64(10)	C29	C27	C28	117.9(3)
O6	Tb1	O2	144.81(10)	O1	C28	Tb1	60.37(19)
O6	Tb1	O8	145.54(11)	O1	C28	C27	122.0(3)
O6	Tb1	O9	70.65(10)	O1	C28	O2	118.6(3)
O6	Tb1	O7	76.20(11)	C27	C28	Tb1	160.4(3)
O5	Tb1	O6	77.43(10)	O2	C28	Tb1	60.87(19)
O5	Tb1	O1	158.55(10)	O2	C28	C27	119.3(3)
O5	Tb1	C28	150.40(10)	C21	N14	C222	125.6(3)
O5	Tb1	O21	78.21(10)	O5	C13	O11	125.1(4)
O5	Tb1	O2	133.46(9)	O5	C13	C14	118.7(3)
O5	Tb1	O8	78.62(10)	O11	C13	C14	116.2(4)
O5	Tb1	O9	124.84(10)	C26	C24	C25	120.5(3)
O5	Tb1	O7	91.00(11)	C26	C24	C23	120.5(3)
O1	Tb1	C28	25.92(10)	C23	C24	C25	119.0(3)
O1	Tb1	O2	51.47(8)	Tb11	O2	Tb1	114.65(10)
O21	Tb1	O1	115.46(9)	C28	O2	Tb11	152.3(2)
O2	Tb1	C28	26.31(10)	C28	O2	Tb1	92.8(2)
O21	Tb1	C28	91.60(10)	C14	C20	C19	119.7(3)
O21	Tb1	O2	65.35(10)	C21	N23	C19	125.7(3)
O21	Tb1	O9	78.48(10)	C20	C14	C13	119.9(3)
O8	Tb1	O1	87.11(10)	C15	C14	C13	119.2(3)
O8	Tb1	C28	72.30(11)	C15	C14	C20	120.8(3)
O8	Tb1	O2	68.19(10)	C22	C29	C27	120.5(3)
O8	Tb1	O21	80.77(10)	O12	C21	N14	123.4(3)
O8	Tb1	O9	143.79(10)	O12	C21	N23	124.0(4)
O8	Tb1	O7	79.83(11)	N23	C21	N14	112.6(3)
O9	Tb1	O1	75.66(10)	O4	C25	C24	119.5(3)
O9	Tb1	C28	78.94(10)	O4	C25	O3	122.9(3)
O9	Tb1	O2	76.24(9)	O3	C25	C24	117.5(3)
O7	Tb1	O1	70.60(10)	C24	C23	C22	120.2(3)

O7	Tb1	C28	89.26(11)	C16	C18	C19	119.6(3)
O7	Tb1	O2	113.16(10)	C14	C15	C16	119.3(4)
O7	Tb1	O21	159.33(11)	C18	C16	C173	121.0(3)
O7	Tb1	O9	121.87(11)	C15	C16	C18	120.7(4)
C24	C26	C27	118.9(3)	C15	C16	C173	118.2(4)
C17	O6	Tb1	169.2(3)	O6	C17	C164	120.1(3)
C13	O5	Tb1	151.2(3)	O6	C17	O10	123.2(4)
C28	O1	Tb1	93.7(2)	O10	C17	C164	116.7(4)
C20	C19	N23	123.3(3)	N145	C22	C23	123.4(3)
C18	C19	C20	119.7(4)	C29	C22	N145	117.5(3)
C18	C19	N23	116.9(3)	C29	C22	C23	119.1(3)

[1]2-X,-Y,-Z; [2]-1/2+X,-1/2-Y,-1/2+Z; [3]-1/2+X,1/2-Y,-1/2+Z; [4]1/2+X,1/2-Y,1/2+Z; [5]1/2+X,-1/2-Y,1/2+Z

References

[1] (a) Q. Zhu, C. Shen, C. Tan, T. Sheng, S. Hu and X. Wu, *Chem. Commun.*, 2012, **48**, 531–533; (b) J. C. Mello, H. F. Wittmann and R. H. Friend, *Adv. Mater.*, 1997, **9**, 230–232; (c) H. B. Zhang , L. J. Zhou , J. Wei , Z. H. Li , P. Lin and S. W. Du , *J. Mater. Chem.*, 2012, **22**, 21210-21217.

[2] G. M. Sheldrick, A short history of SHELX, *Acta Crystallogr. Sect. A*, 2008, **64**, 112-122.